

We are IntechOpen, the world's leading publisher of Open Access books Built by scientists, for scientists

6,900

Open access books available

185,000

International authors and editors

200M

Downloads

Our authors are among the

154

Countries delivered to

TOP 1%

most cited scientists

12.2%

Contributors from top 500 universities



WEB OF SCIENCE™

Selection of our books indexed in the Book Citation Index
in Web of Science™ Core Collection (BKCI)

Interested in publishing with us?
Contact book.department@intechopen.com

Numbers displayed above are based on latest data collected.
For more information visit www.intechopen.com



A Robust Decoupling Estimator to Identify Electrical Parameters for Three-Phase Permanent Magnet Synchronous Motors

Paolo Mercorelli

*Faculty of Automotive Engineering, Ostfalia University of Applied Sciences
Germany*

1. Introduction

As the high field strength neodymium-iron-boron (NdFeB) magnets become commercially available and affordable, the sinusoidal back electromotive force (emf) permanent magnet synchronous motors (PMSMs) are receiving increasing attention due to their high speed, high power density and high efficiency. These characteristics are very favourable for high performance applications, e.g., robotics, aerospace, and electric ship propulsion systems Rahman et al. (1996), Ooshima et al. (2004). PMSMs as traction motors are common in electric or hybrid road vehicles, but not yet widely used for rail vehicles. Although the traction PMSM has many advantages, just a few prototypes of vehicles were built and tested. The following two new prototypes of rail vehicles with traction PMSMs, which were presented at the InnoTrans fair in Berlin 2008, were the Alstom AGV high speed train and the Skoda Transportation low floor tram 15T ForCity. The greatest advantage of the PMSM is its low volume in contrast to other types of motors, which makes a direct drive of wheels possible. However, the traction drive with PMSM must meet special requirements typical for overhead-line-fed vehicles. The drives and especially their control should be robust to a wide range of overhead line voltage tolerance (typically from -30% to $+20\%$), voltage surges and input filter oscillations. These features may cause problems during flux weakening operation, which must be used for several reasons. The typical reason is to obtain constant power operation in a wide speed range and to reach nominal power during low speed (commonly $1/3$ of the maximum speed). In the case of common traction motors such as asynchronous or DC motors, it is possible to reach the constant power region using flux weakening. This is also possible for traction PMSM, however, a problem with high back emf arises. In the report by Dolecek (2009), the usage of a flux weakening control strategy for PMSM as a prediction control structure is shown to improve the dynamic performance of traditional feedback control strategies. This is obtained in terms, for instance, of overshoot and rising time. It is known that, an accurate knowledge of the model and its parameters is necessary for realizing an effective prediction control. To achieve desired system performance, advanced control systems are usually required to provide fast and accurate response, quick disturbance recovery and parameter variations insensitivity Rahman et al. (2003). Acquiring accurate models for systems under investigation is usually the fundamental part in advanced control system designs. For instance, proper implementation of flux weakening control requires the knowledge of synchronous machine parameters. The most

common parameters required for the implementation of such advanced control algorithms are the classical simplified model parameters: L_d - the direct axis self-inductance, L_q - the quadrature axis self-inductance, and Φ - the permanent magnet flux linkage. Prior knowledge of the previously mentioned parameters and the number of pole pairs p allows for the implementation of torque control through the use of current vector control. Techniques have been proposed for the parameters' identification of PMSM from different perspectives, such as offline Kiltathau et al. (2002), Weisgerber et al. (1997) and online identification of PMSM electrical parameters Mobarakeh et al. (2001), Khaburi et al. (2003). These techniques are based on the decoupled control of linear systems when the motor's mechanical dynamics are ignored. Using a decoupling control strategy, internal dynamics may be almost obscured, but it is useful to remember that there are no limitations in the controllability and observability of the system. In the report by Mercorelli et al. (2003) a decoupling technique is used to control a permanent magnets machine more efficiently in a sensorless way using an observer. The work described by Liu et al. (2008) investigates the possibility of using a numerical approach Particle Swarm Optimization (PSO) as a promising alternative. PSO approach uses a system with a known model structure but unknown parameters. The parameter identification problem can be treated as an optimisation problem, involving comparison of the system output with the model output. The discrepancy between the system and model outputs is minimised by optimisation based on a fitness function, which is defined as a measure of how well the model output fits the measured system output. This approach utilises numerical techniques for the optimisation, and it can incur in difficult non-convex optimisation problems because of the nonlinearity of the motor model. Despite limitation on the frequency range of identification, this paper proposes a dynamic observer based on an optimised decoupling technique to estimate L_{dq} and R_s parameters. The proposed optimisation technique, similar to that presented by Mercorelli (2009) applies a procedure based on minimum variance error to minimise the effects of non-exact cancellation due to the decoupling controller. In the meantime, the paper proposes a particular observer that identifies the permanent magnet flux using the estimated L_{dq} and R_s parameters. The whole structure of the observer is totally new. The limit of this observer for the estimation of the permanent magnet flux is given by the range of work frequency. In fact, examining the theoretical structure of the observer, these limits appear evident and are validated with simulated data, as the estimation becomes inaccurate for low and high velocity of the motor. Because of the coupled nonlinear system structure, a general expression of limits is not easy to find. The paper is organised in the following way: a sketch of the model of the synchronous motor and its behaviour are given in Section 2, Section 3 is devoted to deriving, proposing and discussing the dynamic estimator, and Section 4 shows the simulation results using real data for a three-phase PMSM.

2. Model and behavior of a synchronous motor

To aid advanced controller design for PMSM, it is very important to obtain an appropriate model of the motor. A good model should not only be an accurate representation of system dynamics but should also facilitate the application of existing control techniques. Among a variety of models presented in the literature since the introduction of PMSM, the two-axis dq-model obtained using Park's transformation is the most widely used in variable speed PMSM drive control applications Rahman et al. (2003) and Khaburi et al. (2003). The Park's dq-transformation is a coordinate transformation that converts the three-phase stationary variables into variables in a rotating coordinate system. In dq-transformation, the rotating coordinate is defined relative to a stationary reference angle as illustrated in Fig. 1. The

dq-model is considered in this work.

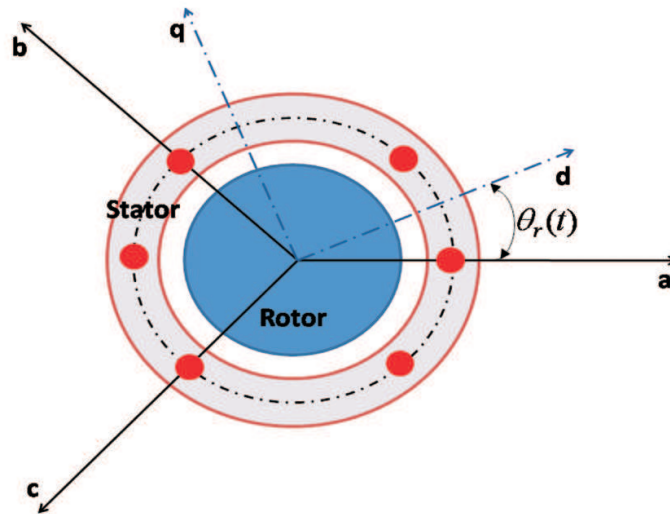


Fig. 1. Park’s transformation for the motor

$$\begin{bmatrix} u_d(t) \\ u_q(t) \\ u_0(t) \end{bmatrix} = \begin{bmatrix} \frac{2 \sin(\omega_{el}t)}{3} & \frac{2 \sin(\omega_{el}t-2\pi/3)}{3} & \frac{2 \sin(\omega_{el}t+2\pi/3)}{3} \\ \frac{2 \cos(\omega_{el}t)}{3} & \frac{2 \cos(\omega_{el}t-2\pi/3)}{3} & \frac{2 \cos(\omega_{el}t+2\pi/3)}{3} \\ \frac{1}{3} & \frac{1}{3} & \frac{1}{3} \end{bmatrix} \begin{bmatrix} u_a(t) \\ u_b(t) \\ u_c(t) \end{bmatrix}, \quad (1)$$

$$\begin{bmatrix} i_d(t) \\ i_q(t) \\ i_0(t) \end{bmatrix} = \begin{bmatrix} \frac{2 \cos(\omega_{el}t)}{3} & \frac{2 \cos(\omega_{el}t-2\pi/3)}{3} & \frac{2 \cos(\omega_{el}t+2\pi/3)}{3} \\ -\frac{2 \sin(\omega_{el}t)}{3} & -\frac{2 \sin(\omega_{el}t-2\pi/3)}{3} & -\frac{2 \sin(\omega_{el}t+2\pi/3)}{3} \\ \frac{1}{3} & \frac{1}{3} & \frac{1}{3} \end{bmatrix} \begin{bmatrix} i_a(t) \\ i_b(t) \\ i_c(t) \end{bmatrix}. \quad (2)$$

The dynamic model of the synchronous motor in d-q-coordinates can be represented as follows:

$$\begin{bmatrix} \frac{di_d(t)}{dt} \\ \frac{di_q(t)}{dt} \end{bmatrix} = \begin{bmatrix} -\frac{R_s}{L_d} & \frac{L_q}{L_d} \omega_{el}(t) \\ -\frac{R_s}{L_q} & -\frac{L_d}{L_q} \omega_{el}(t) \end{bmatrix} \begin{bmatrix} i_d(t) \\ i_q(t) \end{bmatrix} + \begin{bmatrix} \frac{1}{L_d} & 0 \\ 0 & \frac{1}{L_q} \end{bmatrix} \begin{bmatrix} u_d(t) \\ u_q(t) \end{bmatrix} - \begin{bmatrix} 0 \\ \Phi \omega_{el}(t) \end{bmatrix}, \quad (3)$$

and

$$M_m = \frac{3}{2} p \{ \Phi i_q(t) + (L_d - L_q) i_d(t) i_q(t) \}. \quad (4)$$

In (3) and (4), $i_d(t)$, $i_q(t)$, $u_d(t)$ and $u_q(t)$ are the dq-components of the stator currents and voltages in synchronously rotating rotor reference frame, $\omega_{el}(t)$ is the rotor electrical angular speed, the parameters R_s , L_d , L_q , Φ and p are the stator resistance, d-axis and q-axis inductance, the amplitude of the permanent magnet flux linkage, and p the number of couples of permanent magnets, respectively. At the end, M_m indicates the motor torque. Considering an isotropic motor with $L_d \simeq L_q = L_{dq}$, it follows:

$$\begin{bmatrix} \frac{di_d(t)}{dt} \\ \frac{di_q(t)}{dt} \end{bmatrix} = \begin{bmatrix} -\frac{R_s}{L_{dq}} & \omega_{el}(t) \\ -\frac{R_s}{L_{dq}} & \omega_{el}(t) \end{bmatrix} \begin{bmatrix} i_d(t) \\ i_q(t) \end{bmatrix} + \begin{bmatrix} \frac{1}{L_{dq}} & 0 \\ 0 & \frac{1}{L_{dq}} \end{bmatrix} \begin{bmatrix} u_d(t) \\ u_q(t) \end{bmatrix} - \begin{bmatrix} 0 \\ \Phi \omega_{el}(t) \end{bmatrix}, \quad (5)$$

and

$$M_m = \frac{3}{2} p \Phi i_q(t), \quad (6)$$

with the following movement equation:

$$M_m - M_w = J \frac{d\omega_{mec}(t)}{dt}, \tag{7}$$

where $p\omega_{mech}(t) = \omega_{el}(t)$ and M_w is an unknown mechanical load.

3. Structure of the decoupling dynamic estimator

The present estimator uses the measurements of input voltages, currents and angular velocity of the motor to estimate the "d-q" winding inductance, the rotor resistance and amplitude of the linkage flux. The structure of the estimator is described in Fig. 2. This diagram shows how the estimator works. In particular, after having decoupled the system described in (5), the stator resistance R_s and the inductance L_{dq} are estimated through a minimum error variance approach. The estimated values \hat{R}_s and \hat{L}_{dq} are used for to estimate of the amplitude of the linkage flux ($\hat{\Phi}$).

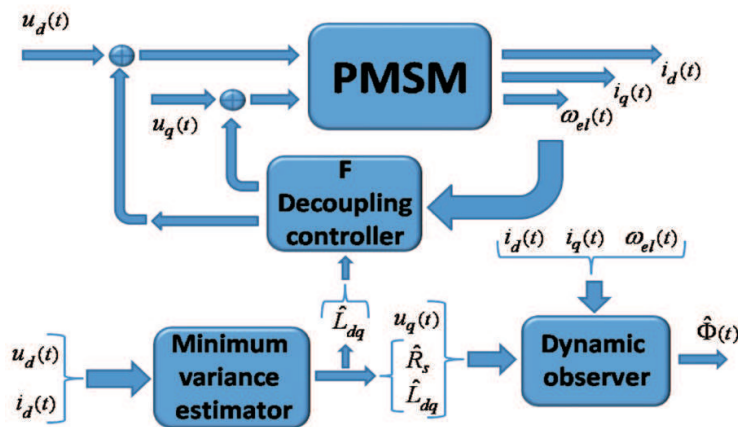


Fig. 2. Conceptual structure of the whole estimator

3.1 Decoupling structure and minimum error variance algorithm

To achieve a decoupled structure of the system described in Eq. (5), a matrix \mathbf{F} is to be calculated such that,

$$(\mathbf{A} + \mathbf{BF})\mathcal{V} \subseteq \mathcal{V}, \tag{8}$$

where $\mathbf{u}(t) = \mathbf{F}\mathbf{x}(t)$ is a state feedback with $\mathbf{u}(t) = [u_d(t), u_q(t)]^T$ and $\mathbf{x}(t) = [i_d(t), i_q(t)]^T$,

$$\mathbf{A} = \begin{bmatrix} -\frac{R_s}{L_{dq}} & \omega_{el}(t) \\ -\frac{R_s}{L_{dq}} & \omega_{el}(t) \end{bmatrix}, \mathbf{B} = \begin{bmatrix} \frac{1}{L_{dq}} & 0 \\ 0 & \frac{1}{L_{dq}} \end{bmatrix}, \tag{9}$$

and $\mathcal{V} = im([0, 1]^T)$ of Eq. (8), according to Basile et al. (1992), is a controlled invariant subspace. More explicitly it follows:

$$\mathbf{F} = \begin{bmatrix} F_{11} & F_{12} \\ F_{21} & F_{22} \end{bmatrix}, \text{ and } \begin{bmatrix} u_d(t) \\ u_q(t) \end{bmatrix} = \mathbf{F} \begin{bmatrix} i_d(t) \\ i_q(t) \end{bmatrix},$$

then the decoupling of the dynamics is obtained via the following relationship:

$$\text{im} \left(\begin{bmatrix} -\frac{R_s}{L_{dq}} \omega_{el}(t) \\ -\frac{R_s}{L_{dq}} \omega_{el}(t) \end{bmatrix} \right) + \text{im} \left(\begin{bmatrix} \frac{1}{L_{dq}} & 0 \\ 0 & \frac{1}{L_{dq}} \end{bmatrix} \begin{bmatrix} F_{11} & F_{12} \\ F_{21} & F_{22} \end{bmatrix} \begin{bmatrix} 0 \\ 1 \end{bmatrix} \right) \subseteq \text{im} \begin{bmatrix} 0 \\ 1 \end{bmatrix}, \quad (10)$$

where the parameters F_{11}, F_{12}, F_{21} , and F_{22} are to be calculated in order to guarantee condition (10) and a suitable dynamics for sake of estimation. Condition (10) is guaranteed if

$$F_{12} = -\omega_{el}(t)L_{dq}. \quad (11)$$

$$\frac{di_d(t)}{dt} = -\frac{R_s}{L_{dq}}i_d(t) + \frac{u_d(t)}{L_{dq}}, \quad (12)$$

Because of the possible inexact decoupling, it follows that:

$$\frac{d\hat{i}_d(t)}{dt} = -\frac{R_s}{L_{dq}}\hat{i}_d(t) + \frac{u_d(t)}{L_{dq}} + n(\Delta(\omega_{el}(t)(L_{dq} - \hat{L}_{dq}))), \quad (13)$$

where $n(\Delta(L_{dq} - \hat{L}_{dq}))$ is the disturbance due to the inexact cancelation.

Proposition 1. Considering the disturbance $n(\Delta(L_{dq} - \hat{L}_{dq}))$ of Eq. (12) as a white noise, then the current minimum variance error $\sigma(e_{i_d}(t)) = \sigma(i_d(t) - \hat{i}_d(t))$ is obtained by minimising the estimation error of the parameters L_{dq} and R_s .

Proof 1. If Eqs. (12) and (13) are discretised using Implicit Euler with a sampling frequency equal to t_s , then it follows that:

$$\hat{i}_d(k) = \frac{\hat{i}_d(k-1)}{(1 + t_s \frac{R_s}{L_{dq}})} + \frac{t_s}{L_{dq}(1 + t_s \frac{R_s}{L_{dq}})} u_d(k), \quad (14)$$

$$\hat{i}_d(k) = \frac{\hat{i}_d(k-1)}{(1 + t_s \frac{R_s}{L_{dq}})} + \frac{t_s}{L_{dq}(1 + t_s \frac{R_s}{L_{dq}})} u_d(k) + n(k). \quad (15)$$

It is possible to assume an ARMAX model for the system represented by (15) and thus

$$i_d(k) = \hat{i}_d(k) + a_1\hat{i}_d(k-1) + a_2\hat{i}_d(k-2) + b_1u_d(k-1) + b_2u_d(k-2) + n(k) + c_{1u}n(k-1) + c_{2u}n(k-2). \quad (16)$$

Letting $e_{i_d}(k) = i_d(k) - \hat{i}_d(k)$ as mentioned above, it follows that:

$$e_{i_d}(k) = a_1\hat{i}_d(k-1) + a_2\hat{i}_d(k-2) + b_1u_d(k-1) + b_2u_d(k-2) + n(k) + c_1n(k-1) + c_2n(k-2), \quad (17)$$

where the coefficients a, b, c_1, c_2 , are to be estimated, and $n(k)$ is assumed as white noises. The next sample is:

$$e_{i_d}(k+1) = a_1\hat{i}_d(k) + a_2\hat{i}_d(k-1) + b_1u_d(k) + b_2u_d(k-1) + n(k+1) + c_1n(k) + c_2n(k-1). \quad (18)$$

The prediction at time "k" is:

$$\hat{e}_{i_d}(k+1/k) = a_1\hat{i}_d(k) + a_2\hat{i}_d(k-1) + b_1u_d(k) + b_2u_d(k-1) + c_1n(k) + c_2n(k-1). \quad (19)$$

Considering that:

$$J = E\{e_{i_d}^2(k+1/k)\} = E\{[\hat{e}_{i_d}(k+1/k) + n(k+1)]^2\},$$

and assuming that the noise is not correlated to the signal $e_{i_d}(k)$, it follows:

$$E\{[\hat{e}_{i_d}(k+1/k) + n(k+1)]^2\} = E\{[\hat{e}_{i_d}(k+1/k)]^2\} + E\{[n(k+1)]^2\} = E\{[\hat{e}_{i_d}(k+1/k)]^2\} + \sigma_n^2, \quad (20)$$

where σ_n is defined as the variance of the white noises. The goal is to find $\hat{i}_d(k)$ such that:

$$\hat{e}_{i_d}(k+1/k) = 0. \quad (21)$$

It is possible to write (17) as

$$n(k) = e_{i_d}(k) - a_1\hat{i}_d(k-1) - a_2\hat{i}_d(k-2) - b_1u_d(k-1) - b_2u_d(k-2) - c_1n(k-1) - c_2n(k-2). \quad (22)$$

Considering the effect of the noise on the system as follows:

$$c_1n(k-1) + c_2n(k-2) \approx c_1n(k-1), \quad (23)$$

and using the Z-transform, then:

$$N(z) = \hat{I}_d(z) - a_1z^{-1}\hat{I}_d(z) - a_2z^{-2}\hat{I}_d(z) - b_1z^{-1}U_d(z) - b_2z^{-2}U_d(z) - c_1z^{-1}N(z) \quad (24)$$

and

$$N(z) = \frac{(1 - a_1z^{-1} - a_2z^{-2})}{1 + c_1z^{-1}}\hat{I}_d(z) - \frac{(b_1z^{-1} + b_2z^{-2})}{1 + c_1z^{-1}}U_d(z). \quad (25)$$

Inserting Eq. (25) into Eq. (19) after its Z-transform, and considering the approximation stated in (23) and Eq. (21), the following expression is obtained:

$$\hat{I}_d(z) = -\frac{(a_1 + c_1 + b_1z^{-1})}{b_1(1 + c_1z^{-1}) + b_2(1 + c_1z^{-1})}U_d(z). \quad (26)$$

Using the Z-transform for Eq. (14) it follows:

$$I_d(z) = \frac{t_s}{L_{dq} + t_sR_s - L_{dq}z^{-1}}U_d(z). \quad (27)$$

Comparing (26) with (27), we are left with a straightforward diophantine equation to solve. The diophantine equation gives the relationship between the parameters $\Theta = [a_1, b_1, b_2, c_1]$ as follows:

$$-b_1 = 0 \quad (28)$$

$$a_1 + c_1 = t_s \quad (29)$$

$$b_1 + b_2 = L_{dq} + t_sR_s \quad (30)$$

$$b_1c_1 + b_2c_1 = -L_{dq}. \quad (31)$$

Guessed initial values for parameters L_{dq} , R_s are given. This yields initial values for the parameters $\Theta = [a_1, b_1, b_2, c_1]$. New values for the vector Θ are calculated using the recursive least squares method. \square

Remark 1. The approximation in equation (23) is equivalent to considering $\|c_2\| \ll \|c_1\|$. In other words, this means that a noise model of the first order is assumed. An indirect validation of this assumption is given by the results. In fact, the final measurements show in general good results with the proposed method. \square

Remark 2. At the end, the recursive least-squares method gives an estimation of the parameters L_{dq} and R_s . These calculated parameters L_{dq} and R_s minimize the current minimum variance error $\sigma(e_{i_d}(t)) = \sigma(i_d(t) - \hat{i}_d(t))$. \square

3.2 The dynamic estimator of Φ

If the electrical part of the system "q" and "d" axes is considered, then, assuming that $\omega_{el}(t) \neq 0$, $i_q(t) \neq 0$, and $i_d(t) \neq 0$, the following equation can be considered:

$$\Phi(t) = -\frac{L_{dq} \frac{di_q(t)}{dt} + R_s i_d(t) + L_{dq} \omega_{el}(t) i_q(t) + u_q(t)}{\omega_{el}(t)}. \quad (32)$$

Consider the following dynamic system:

$$\frac{d\hat{\Phi}(t)}{dt} = -\mathcal{K}\hat{\Phi}(t) - \mathcal{K} \left(\frac{\hat{L}_{dq} \frac{di_q(t)}{dt} + \hat{R}_s i_d(t)}{\omega_{el}(t)} + \frac{\hat{L}_{dq} \omega_{el}(t) i_q(t) + u_q(t)}{\omega_{el}(t)} \right), \quad (33)$$

where \mathcal{K} is a function to be calculated. Eq. (33) represents the estimators of Φ . If the error functions are defined as the differences between the true and the observed values, then:

$$e_{\Phi}(t) = \Phi(t) - \hat{\Phi}(t), \quad (34)$$

and

$$\frac{de_{\Phi}(t)}{dt} = \frac{d\Phi(t)}{dt} - \frac{d\hat{\Phi}(t)}{dt}. \quad (35)$$

If the following assumption is given:

$$\left\| \frac{d\Phi(t)}{dt} \right\| \ll \left\| \frac{d\hat{\Phi}(t)}{dt} \right\|, \quad (36)$$

then in Eq. (35), the term $\frac{d\Phi(t)}{dt}$ is negligible. Using equation (33), Eq. (35) becomes

$$\frac{de_{\Phi}(t)}{dt} = \mathcal{K}\hat{\Phi}(t) + \mathcal{K}_3 \left(\frac{\hat{L}_{dq} \frac{di_q(t)}{dt} + \hat{R}_s i_d(t)}{\omega_{el}(t)} + \frac{\hat{L}_{dq} \omega_{el}(t) i_q(t) + u_q(t)}{\omega_{el}(t)} \right). \quad (37)$$

Because of Eq. (32), (37) can be written as follows:

$$\frac{de_{\Phi}(t)}{dt} = \mathcal{K}\hat{\Phi}(t) - \mathcal{K}\Phi(t), \quad (38)$$

and considering (34), then

$$\frac{de_{\Phi}(t)}{dt} + \mathcal{K}\Phi(t) = 0. \quad (39)$$

\mathcal{K} can be chosen to make Eq. (39) exponentially stable. To guarantee exponential stability, \mathcal{K} must be

$$\mathcal{K} > 0.$$

To guarantee $\|\frac{d\Phi(t)}{dt}\| \ll \|\frac{d\hat{\Phi}(t)}{dt}\|$, then $\mathcal{K} \gg 0$. The observer defined in (33) suffers from the presence of the derivative of the measured current. In fact, if measurement noise is present in the measured current, then undesirable spikes are generated by the differentiation. The proposed algorithm must cancel the contribution from the measured current derivative. This is possible by correcting the observed velocity with a function of the measured current, using a supplementary variable defined as

$$\eta(t) = \hat{\Phi}(t) + \mathcal{N}(i_q(t)), \quad (40)$$

where $\mathcal{N}(i_q(t))$ is the function to be designed.

Consider

$$\frac{d\eta(t)}{dt} = \frac{d\Phi(t)}{dt} + \frac{d\mathcal{N}(i_q(t))}{dt} \quad (41)$$

and let

$$\frac{d\mathcal{N}(i_q(t))}{dt} = \frac{d\mathcal{N}(i_q)}{di_q(t)} \frac{di_q(t)}{dt} = \frac{\mathcal{K}\hat{L}_{dq}}{\omega_{el}(t)} \frac{di_q(t)}{dt}. \quad (42)$$

The purpose of (42) is to cancel the differential contribution from (33). In fact, (40) and (41) yield, respectively,

$$\hat{\Phi}(t) = \eta(t) - \mathcal{N}(i_q(t)) \quad \text{and} \quad (43)$$

$$\frac{d\hat{\Phi}(t)}{dt} = \frac{d\eta(t)}{dt} - \frac{d\mathcal{N}(i_q(t))}{dt}. \quad (44)$$

Substituting (42) in (44) results in

$$\frac{d\hat{\Phi}(t)}{dt} = \frac{d\eta(t)}{dt} - \frac{\mathcal{K}\hat{L}_{dq}}{\omega_{el}(t)} \frac{di_q(t)}{dt}. \quad (45)$$

Inserting Eq. (45) into Eq. (33), the following expression is obtained¹:

$$\frac{d\eta(t)}{dt} - \frac{\mathcal{K}\hat{L}_{dq}}{\omega_{el}(t)} \frac{di_q(t)}{dt} = -\mathcal{K}\hat{\Phi}(t) - \mathcal{K} \left(\frac{\hat{L}_{dq} \frac{di_q(t)}{dt} + \hat{R}_s i_d(t)}{\omega_{el}(t)} + \frac{\hat{L}_{dq} \omega_{el}(t) i_q(t) + u_q(t)}{\omega_{el}(t)} \right), \quad (46)$$

then

$$\frac{d\eta(t)}{dt} = -\mathcal{K}\hat{\Phi}(t) - \mathcal{K} \frac{(\hat{R}_s i_d(t) + \hat{L}_{dq} \omega_{el}(t) i_q(t) + u_q(t))}{\omega_{el}(t)}. \quad (47)$$

Letting $\mathcal{N}(i_q(t)) = k_{app} i_q(t)$, where a parameter has been indicated with k_{app} , then from (42) $\Rightarrow \mathcal{K} = \frac{k_{app} \omega_{el}(t)}{\hat{L}_{dq}}$, and Eq. (43) becomes:

$$\hat{\Phi}(t) = \eta(t) - k_{app} i_q(t). \quad (48)$$

Finally, substituting (48) into (47) results in the following equation:

$$\frac{d\eta(t)}{dt} = -\frac{k_{app} \omega_{el}(t)}{\hat{L}_{dq}} (\eta(t) - k_{app} i_q(t)) + \frac{k_{app}}{\hat{L}_{dq}} (\hat{R}_s i_d(t) + \hat{L}_{dq} \omega_{el}(t) i_q(t) + u_q(t)),$$

$$\hat{\Phi}(t) = \eta(t) - k_{app} i_q(t). \quad (49)$$

¹ Expression (33) works under the assumption (36): fast observer dynamics.

Using the implicit Euler method, the following velocity observer structure is obtained:

$$\eta(k) = \frac{\eta(k-1)}{1 + t_s \frac{k_{app} \omega_{el}(k)}{\hat{L}_{dq}}} + \frac{t_s \frac{k_{app}^2 \omega_{el}(k) i_q(k)}{\hat{L}_{dq}} + k_{app} \omega_{el}(k) i_q(k) + \frac{t_s \hat{R}_s k_{app} i_d(k)}{\hat{L}_{dq}}}{1 + t_s \frac{k_{app} \omega_{el}(k)}{\hat{L}_{dq}}} i_q(k) + \frac{t_s \frac{k_{app}}{\hat{L}_{dq}}}{1 + t_s \frac{k_{app} \omega_{el}(k)}{\hat{L}_{dq}}} u_q(k),$$

$$\hat{\Phi}(k) = \eta(k) - k_{app} i_q(k), \tag{50}$$

where t_s is the sampling period.

Remark 3. Assumption (36) states that the dynamics of the approximating observer should be faster than the dynamics of the physical system. This assumption is typical for the design of observers. □

Remark 4. The estimator of Eq. (50) presents the following limitations: for low velocity of the motor ($\omega_{mec}(t) \ll \omega_{mec_n}(t)$), where $\omega_{mec_n}(t)$ represents the nominal velocity of the motor), the estimation of Φ becomes inaccurate. Because $\omega_{el}(t)$ divides the state variable η , the observer described by (50) becomes hyperdynamic. Critical phases of the estimation are the starting and ending of the movement. Another critical phase is represented by high velocity regime. In fact, it has been proven through simulations that if $\omega_{mec}(t) \gg \omega_{mec_n}(t)$, then the observer described by (50) becomes hypodynamic. According to the simulation results, within some range of frequency, this hypo-dynamicity can be compensated by a suitable choice of k_{app} . □

Remark 5. The Implicit Euler method guarantees the finite time convergence of the observer for any choice of k_{app} . Nevertheless, any other method can demonstrate the validity of the presented results. Implicit Euler method is a straightforward one. □

4. Simulation results

Simulations have been performed using a special stand with a 58-kW traction PMSM. The stand consists of a PMSM, a tram wheel and a continuous rail. The PMSM is a prototype for low floor trams. The PMSM parameters are: nominal power 58 kW, nominal torque 852 Nm, nominal speed 650 rpm, nominal phase current 122 A and number of poles 44. The model parameters are: $R = 0.08723$ Ohm, $L_{dq} = L_d = L_q = 0.8$ mH, $\Phi = 0.167$ Wb. Surface mounted NdFe magnets are used in PMSM. The advantage of these magnets is their inductance, which is as great as 1.2 T, but their disadvantage is corrosion. The PMSM was designed to meet B curve requirements. The stand was loaded by an asynchronous motor. The engine has a nominal power 55 kW, a nominal voltage 380 V and nominal speed 589 rpm. Figures 3, 4, and 5 show the estimation of R_s stator resistance, L_{dq} inductance, and Φ magnet flux, respectively. These simulation results are obtained using values of k_{app} equal to 2 and 20 respectively. From these results, in particular from flux estimation, an improvement, passing from values of $k_{app} = 2$ $k_{app} = 20$, is visible. From these figures, the effect of the limit of the procedure discussed in remark 4 is visible at the beginning of the estimation. Figure 6 shows the angular velocity of the motor. In the present simulations, $t = 0$ corresponds to $\omega_{el}(t) = 0$.

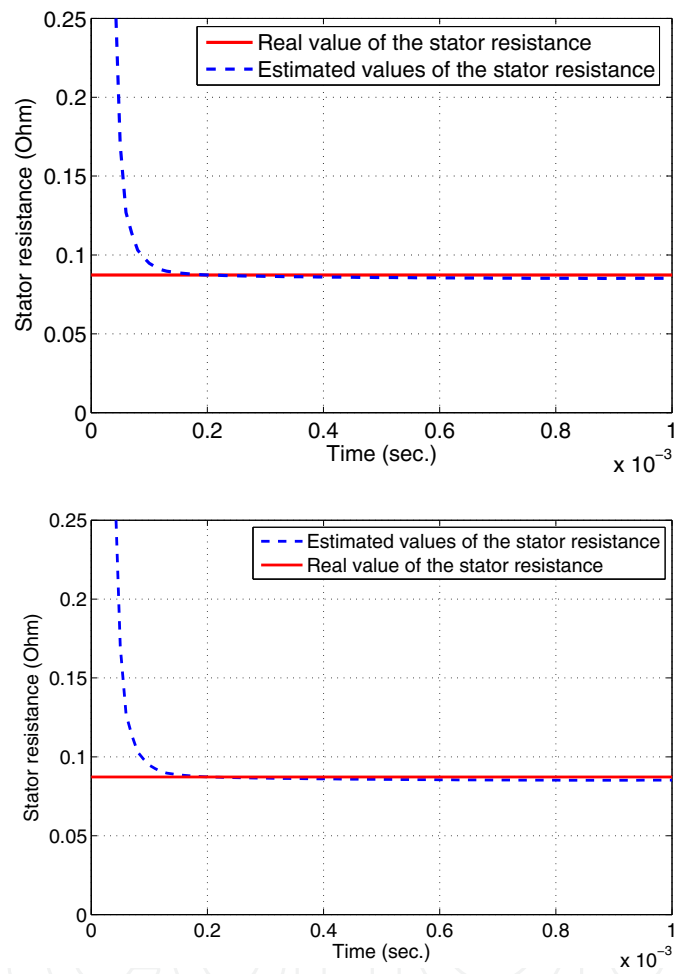


Fig. 3. Estimated and real values of R_s stator resistance for $k_{app} = 2$ (on the top) and $k_{app} = 20$ (on the bottom)

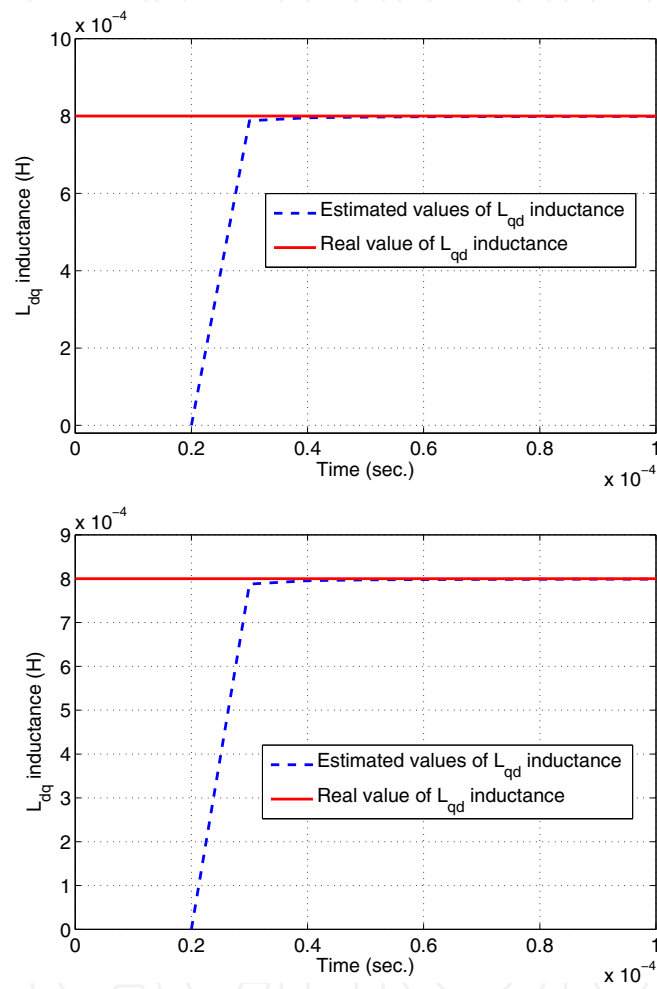


Fig. 4. Estimated and real values of L_{dq} inductance for $k_{app} = 2$ (on the top) and $k_{app} = 20$ (on the bottom)

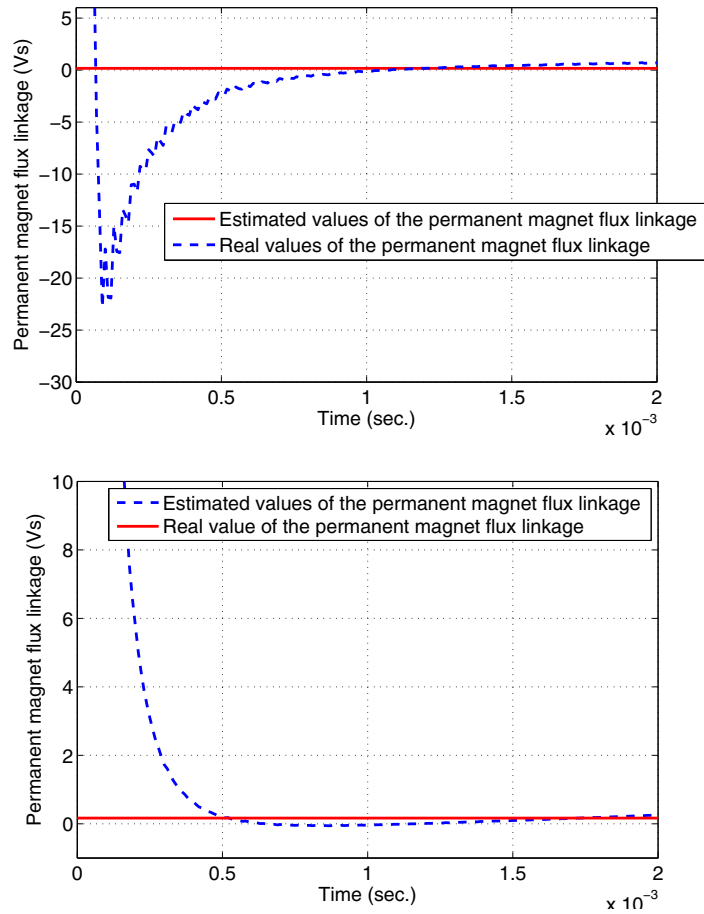


Fig. 5. Estimated and real values of the permanent magnet flux linkage for $k_{app} = 2$ (on the top) and $k_{app} = 20$ (on the bottom)

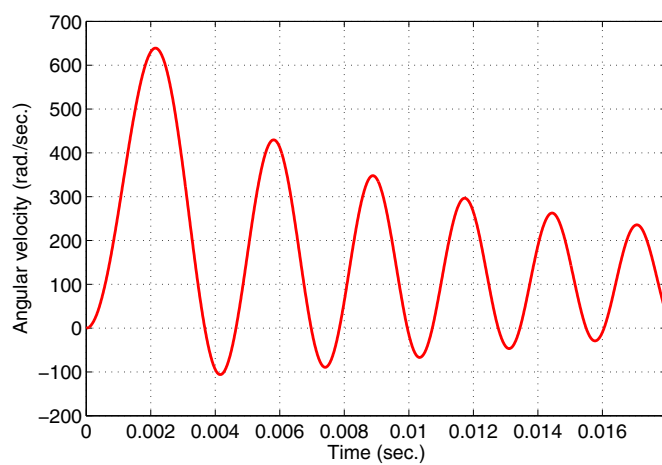


Fig. 6. Angular velocity

5. Conclusions and future work

This paper considers a dynamic estimator for fully automated parameters identification for three-phase synchronous motors. The technique uses a decoupling procedure optimised by a minimum variance error to estimate the inductance and resistance of the motor. Moreover, a dynamic estimator is shown to identify the amplitude of the linkage flux using the estimated inductance and resistance. It is generally applicable and could also be used for the estimation of mechanical load and other types of electrical motors, as well as for dynamic systems with similar nonlinear model structure. Through simulations of a synchronous motor used in automotive applications, this paper verifies the effectiveness of the proposed method in identification of PMSM model parameters and discusses the limits of the found theoretical and the simulation results. Future work includes the estimation of a mechanical load and the general test of the present algorithm using a real motor.

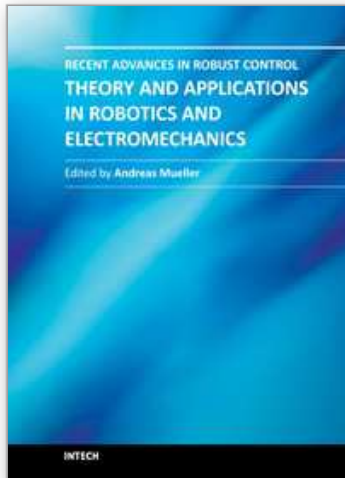
6. References

- G. Basile and G. Marro. "Controlled and conditioned invariants in linear system theory", New Jersey-USA, Prentice Hall, 1992.
- R. Dolecek, J. Novak, and O. Cerny. "Traction Permanent Magnet Synchronous Motor Torque Control with Flux Weakening", *Radioengineering*, Vol. 18, No. 4, December 2009
- D.A. Khaburi and M. Shahnazari. "Parameters Identification of Permanent Magnet Synchronous Machine in Vector Control", in *Proc. of the 10th European Conference on Power Electronics and Applications, EPE 2003, Toulouse, France, 2-4 Sep. 2003*.
- A. Kiltbau, and J. Pacas. "Appropriate models for the controls of the synchronous reluctance machine", in *Proc. IEEE IAS Annu. Meeting, 2002*, pages 2289-2295.
- Li Liu, Wenxin Liu and David A. Cartes. "Permanent Magnet Synchronous Motor Parameter Identification using Particle Swarm Optimization", *International Journal of Computational Intelligence Research* Vol.4, No.2 (2008), pages 211-218
- P. Mercorelli. "Robust Feedback Linearization Using an Adaptive PD Regulator for a Sensorless Control of a Throttle Valve", *Mechatronics, a Journal of IFAC*, Elsevier Science publishing. DOI: 10.1016/j.mechatronics.2009.08.008, Volume 19, Issue 8, pages 1334-1345, December 2009.
- P. Mercorelli, K. Lehmann and S. Liu. "On Robustness Properties in Permanent Magnet Machine Control Using Decoupling Controller", in *Proc. of the 4th IFAC International Symposium on Robust Control Design, 25th-27th June 2003, Milan (Italy)*.
- B.N. Mobarakeh, F. Meibody-Tabar, and F. M. Sargos. "On-line identification of PMSM electrical parameters based on decoupling control", in *Proc. of the Conf. Rec. IEEE-IAS Annu. Meeting, vol. 1, Chicago, IL, 2001*, pages 266-273.
- M. Ooshima, A. Chiba, A. Rahman and T. Fukao. "An improved control method of buried-type IPM bearingless motors considering magnetic saturation and magnetic pull variation", *IEEE Transactions on Energy Conversion*, vol. 19, no. 3, Sept. 2004, pages 569-575.
- M.A. Rahman and P. Zhou. "Analysis of brushless permanent magnet synchronous motors", *IEEE Trans. Industrial Electronics*, vol. 43, no. 2, 1996, pages 256-267.
- M.A. Rahman, D.M. Vilathgamuwa, M.N. Uddin and T. King-Jet. "Nonlinear control of interior permanent magnet synchronous motor", *IEEE Trans. Industry Applications*, vol. 39, no. 2, 2003, pages 408-416.

- S. Weisgerber, A. Proca, and A. Keyhani. "Estimation of permanent magnet motor parameters", in Proc. of the IEEE Ind. Appl. Soc. Annu. Meeting, New Orleans, LA, Oct. 1997, pp. 29–34.

IntechOpen

IntechOpen



Recent Advances in Robust Control - Theory and Applications in Robotics and Electromechanics

Edited by Dr. Andreas Mueller

ISBN 978-953-307-421-4

Hard cover, 396 pages

Publisher InTech

Published online 21, November, 2011

Published in print edition November, 2011

Robust control has been a topic of active research in the last three decades culminating in H_2/H_∞ and μ design methods followed by research on parametric robustness, initially motivated by Kharitonov's theorem, the extension to non-linear time delay systems, and other more recent methods. The two volumes of Recent Advances in Robust Control give a selective overview of recent theoretical developments and present selected application examples. The volumes comprise 39 contributions covering various theoretical aspects as well as different application areas. The first volume covers selected problems in the theory of robust control and its application to robotic and electromechanical systems. The second volume is dedicated to special topics in robust control and problem specific solutions. Recent Advances in Robust Control will be a valuable reference for those interested in the recent theoretical advances and for researchers working in the broad field of robotics and mechatronics.

How to reference

In order to correctly reference this scholarly work, feel free to copy and paste the following:

Paolo Mercorelli (2011). A Robust Decoupling Estimator to Identify Electrical Parameters for Three-Phase Permanent Magnet Synchronous Motors, Recent Advances in Robust Control - Theory and Applications in Robotics and Electromechanics, Dr. Andreas Mueller (Ed.), ISBN: 978-953-307-421-4, InTech, Available from: <http://www.intechopen.com/books/recent-advances-in-robust-control-theory-and-applications-in-robotics-and-electromechanics/a-robust-decoupling-estimator-to-identify-electrical-parameters-for-three-phase-permanent-magnet-syn>

INTECH
open science | open minds

InTech Europe

University Campus STeP Ri
Slavka Krautzeka 83/A
51000 Rijeka, Croatia
Phone: +385 (51) 770 447
Fax: +385 (51) 686 166
www.intechopen.com

InTech China

Unit 405, Office Block, Hotel Equatorial Shanghai
No.65, Yan An Road (West), Shanghai, 200040, China
中国上海市延安西路65号上海国际贵都大饭店办公楼405单元
Phone: +86-21-62489820
Fax: +86-21-62489821

© 2011 The Author(s). Licensee IntechOpen. This is an open access article distributed under the terms of the [Creative Commons Attribution 3.0 License](#), which permits unrestricted use, distribution, and reproduction in any medium, provided the original work is properly cited.

IntechOpen

IntechOpen